ARTICLE

Investigating deposition sequence during synthesis of Pd/Al_2O_3 catalysts modified with organic monolayers

Received 00th January 20xx,
Accepted 00th January 20xx

DOI: 10.1039/x0xx00000x

Zachary Blanchette[a], Jing Zhang[a], Sadegh Yazdi[b,c], Michael B. Griffin[d], Daniel K. Schwartz[a], J. Will Medlin[a,*]

Modification of supported metal catalysts with self-assembled monolayers (SAMs) has been shown to improve selectivity and turnover frequencies (TOFs) for many catalytic reactions. However, these benefits are often accompanied by a decrease in overall mass activity due to partial blocking of active sites by the monolayers. Therefore, a potential method for increasing site accessibility is to deposit the active metal (e.g., Pd) after deposition of a SAM modifier on the support material. In this work, Pd/Al_2O_3 catalysts were synthesized using both a conventional, "metal-first" sequence in which the phosphonic acid (PA) SAM was deposited on Pd/Al_2O_3 and a "SAM-first" technique in which the ligands were deposited onto the support prior to deposition of the metal. Although metal-first catalysts showed a significant increase in TOF during benzyl alcohol HDO, they exhibited only a modest increase in overall mass activity due to a decrease in the number of active sites. Meanwhile, SAM-first catalysts showed similar improvements in TOF and toluene selectivity but exhibited significantly improved HDO rates compared to metal-first catalysts. The rate increase was attributed to reduced site blocking as evidenced by CO chemisorption measurements. Additionally, analysis of catalysts having high Pd loadings using transmission electron microscopy (TEM) showed that SAM-first catalysts generally resulted in lower average particle sizes than traditionally modified and unmodified catalysts, suggesting that precoating the support surface with PAs changes the way that Pd is deposited during incipient wetness, leading here to improved activity.

1. Introduction

Understanding and modifying the properties of catalytic active sites on supported metal catalysts remains an important area of research in the development of practical catalysts with optimal selectivity and activity.[1,2] For example, hydrodeoxygenation (HDO) of aromatic oxygenates is an important step in biomass upgrading to remove excess oxygen[3] from lignocellulosic bio-oil but is highly dependent on the catalyst used.[4–6]

Metal / metal-oxide catalysts are frequently employed as bifunctional catalysts and have proven to be useful for a wide array of reactions.[7–10] In particular, HDO benefits greatly through the use of these types of catalysts because it combines sites that activate hydrogen with sites that are effective for C-O scission.[11] These catalysts are often noble metals dispersed on a metal oxide or encapsulated in the metal oxide to produce a core/shell material.[5,12–14] However, organic ligands have also been employed to prepare bifunctional catalysts. In addition to the many ways that SAMs can modify catalytic performance, including through electronic effects,[15] alterations to adsorption affinities,[16] steric effects,[17] and the creation of molecular recognition sites,[18,19] SAMs have recently been used to alter the properties of bifunctional catalysts by introducing new characteristics at the interface between the metal and support.[20]

Our group has recently demonstrated that phosphonic acid (PA) self-assembled monolayers (SAMs) can be used to modify supported Pt and Pd catalysts to significantly improve selectivity and activity towards gas-phase HDO of aromatic alcohols and phenolics through the introduction of Brønsted acid sites.[20,21] PA modifications, including chloromethyl phosphonic acid (ClMPA), on Pd/Al_2O_3 catalysts have also shown similar improvement for low-temperature vanillin HDO in ethanol and mixed solvents due to increased Brønsted acidity.[22,23] While this method of modification is effective for both Pt and Pd catalysts, subsequent work suggests that PAs can bind both to metal oxide supports[24,25] and to Pd (and other metals, such as Ni).[26,27] In certain cases (such as ring hydrogenation of furfuryl alcohol[28]), PA modification of Pd sites has been found to lead to improved reaction rates due to favorable H-bonding interactions. In other cases, however, metal modification leads to drastically reduced overall activity due to site-blocking effects.[26] Depositing SAMs before incorporating the metal was

[a] Department of Chemical and Biological Engineering, University of Colorado, Boulder, CO 80303, USA.
[b] Renewable & Sustainable Energy Institute, University of Colorado, Boulder, Colorado 80309, USA.
[c] Materials Science & Engineering Program, University of Colorado, Boulder, Colorado 80309, USA.
[d] Catalytic Carbon Transformation and Scale-up Center, National Renewable Energy Lab, Golden, Colorado 80401, USA.

† Electronic Supplementary Information (ESI) available: See DOI: 10.1039/x0xx00000x

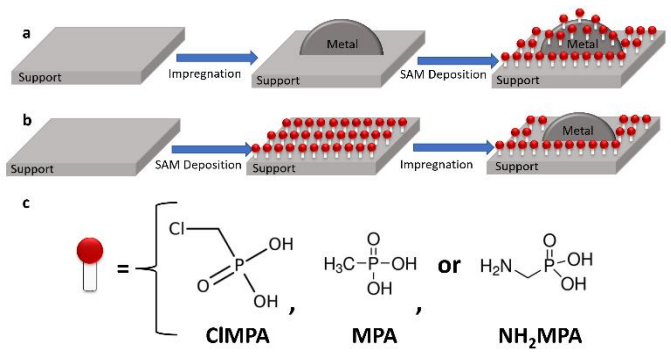

Fig. 1 Schematic representation of catalyst preparation via (a) Metal-First deposition, (b) SAM-First deposition. (c) Structure of phosphonic acids deposited onto the catalysts

found to increase activity; however, the reasons for this increase were not explored in detail.

In this work, we systematically investigated the role of deposition sequence of PA SAMs on HDO activity for Pd/Al_2O_3 catalysts. We synthesized supported Pd catalysts using both a conventional "metal-first" procedure (Fig. 1a) in which Pd/Al_2O_3 was modified by PA SAMs and a reverse "SAM-first" procedure (Fig. 1b) in which the support was modified with PA SAMs prior to metal deposition via incipient wetness impregnation. We hypothesized that the latter approach would promote HDO at the metal-support interface via addition of Brønsted acid sites, while leaving the active metal sites free of poisoning species to retain high activity. The effects of deposition sequence were investigated for various PA SAMs and metal loadings. The hypothetical combined effects of increased selectivity and activity may lead to catalysts that can maximize the production of desired products.

2. Experimental

2.1 Materials & Catalyst Preparation

Aluminum oxide (γ-Al_2O_3, 99.997%), silicon(IV) oxide (SiO_2, 99.9%), methyl phosphonic acid (MPA, 98%), and aminomethyl phosphonic acid (NH_2MPA, 99%) were purchased from Alfa Aesar. Palladium nitrate dihydrate ($Pd(NO_3)_2 \bullet 2H_2O$) and benzyl alcohol (BZA, >99.0%) were purchased from Sigma Aldrich. Chloromethyl phosphonic acid (ClMPA, 98%) was purchased from Frontier Scientific. High-performance liquid chromatography-grade tetrahydrofuran (THF) was purchased from Fisher Chemical. Ultrahigh-purity H_2 and He were purchased form Airgas.

Alumina-supported Pd catalysts were prepared using incipient wetness impregnation. A solution of the metal precursor, $Pd(NO_3)_2 \bullet 2H_2O$, in distilled water was prepared and mixed with the desired mass of support (γ-Al_2O_3) in order to achieve the desired Pd weight loadings of 5 wt%, 1 wt%, and 0.2 wt%. The resulting catalysts were then dried at 120 °C for 6 h to remove any remaining water.

Phosphonic acid SAMs (Fig. 1c) were deposited onto catalysts using a liquid deposition technique reported in prior work.[20,22] First, a 10 mM solution of the acid was prepared using water as the solvent for NH_2MPA and THF as the solvent for ClMPA and MPA. The catalyst was then added to the solution and stirred at ambient conditions for 16 h. The resultant solid was then separated from the solution using centrifugation and annealed at 120 °C for 6 h. The catalyst was then washed with water or THF five times to remove excess PA and vacuum dried overnight at room temperature. This procedure has been shown to produce coverages of 3-5 phosphonates nm^{-2} for most PAs (including ClMPA) on Al_2O_3 and/or Pd/Al_2O_3,[20–22,27] consistent with uniform monolayers.[25,29–32] Using the surface area of 125 m^2 / g provided by the supplier, the approximate loading of the modifiers is 0.62 – 1.04 mmol / g. However, MPA has been found to accumulate to unusually high apparent coverages on a variety of surfaces, e.g. ~8 nm^{-2} (1.66 mmol / g) on $5\%Pd/Al_2O_3$.[20,22,27]

2.2 Material Characterization

Diffuse reflectance infrared Fourier transform (DRIFT) spectra were recorded using a Thermo Fisher Scientific Nicolet 6700 FTIR (100 scans at a resolution of 4 cm^{-1}). Carbon monoxide DRIFTS experiments were performed using the same DRIFTS equipped with a reaction chamber. Prior to CO DRIFTS, the samples were reduced in 20% H_2 at 250 °C for 2 h and purged in argon at 200 °C for 30 min. The sample was then dosed with CO at 50 °C for 20 min and purged with argon at 50 °C for 10 min prior to scanning. Background spectra of the samples prior to CO dosing were subtracted to produce the reported spectra.

CO pulse chemisorption was performed using an Altamira Instruments AMI-300 system equipped with a thermal conductivity detector. Approximately 100 mg of catalyst was loaded into a quartz U-tube reactor and held as a fixed bed on a plug of quartz wool. The sample was pre-treated in 4% H_2/Ar flowing at 50 mL min^{-1} by heating at 10 °C min^{-1} to 250 °C and holding for 2 h. After the pre-treatment, the sample was cooled to 30 °C and flushed with He flowing at 50 mL min^{-1} for 10 min to remove any weakly adsorbed hydrogen. The sample was then exposed to sequential 500 µl pulses of a 10% CO/He gas mixture until saturation. A 500 µl sample loop was used to calibrate the TCD response. Triplicate experiments on an unmodified Pd/Al_2O_3 catalyst indicate a relative standard deviation of 9% on CO uptake and dispersion measurements. A Pd/CO chemisorption stoichiometry of 2 was used for calculating apparent dispersion, as suggested in literature for supported Pd catalysts.[33,34]

High angle annular dark field scanning transmission electron microscopy (HAADF-STEM) images and energy-dispersive X-ray spectroscopy (EDS) maps were obtained using a probe Cs-corrected Thermo Scientific Titan Themis S/TEM equipped with a Super-X detector (four silicon drift detectors) operated at 300 kV. TEM samples were prepared by reducing the catalyst in 20% H_2 at 250 °C for 2 h followed by a helium purge as the sample cooled to room temperature. Catalyst particles were suspended in 5 mL of ethanol creating a solution that was then drop casted onto an ultrathin carbon film on a lacey carbon support film TEM grid. The average metal nanoparticle size and histogram of size distribution were calculated from the HAADF-STEM images

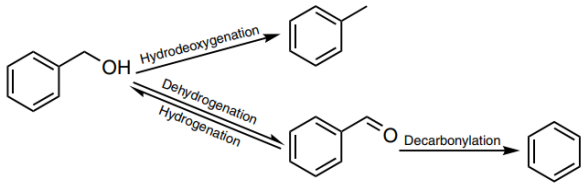

Fig. 2 Benzyl Alcohol hydrodeoxygenation pathway

of 200 particles captured from different locations on the TEM samples. Error for average particle size was estimated using the standard deviation of average particle size in each individual image.

2.3 Kinetic Studies

Prior to catalytic testing, catalysts were reduced in 20% H_2 at 250 °C for 2 h and purged in helium as the temperature decreased to the reaction temperature. The synthesized catalysts were evaluated for HDO of benzyl alcohol (Fig. 2) in a tubular packed bed flow reactor operating at 177 °C and atmospheric pressure. Helium was bubbled through the liquid reactant (benzyl alcohol) heated in a water bath maintained at 53 °C. This stream was combined with H_2 and additional make-up helium prior to reaching the catalyst bed. The resulting stream had gas-phase mole fractions of Y_{H2}=25% and Y_{BZA}=0.053% with a total flowrate of 150 mL/min. The mass of catalyst was controlled to obtain a conversion of 8% ± 2%. The Pd/Al_2O_3 catalyst was with SiO_2 (inactive for benzyl alcohol HDO) to form a 100 mg catalyst bed. Data was taken at 120 min on-stream. The reactor effluent was analyzed using an Agilent 7890A Gas Chromatograph equipped with an Agilent HP-5 capillary column and flame ionization detector. Products were identified via retention time comparisons with standards of known composition. The normalized rate of production was calculated according to Eq 1 by multiplying the product yield ($X_{Toluene}$) by the molar flowrate of benzyl alcohol (F_{BZA}) divided by the effective mass of Pd in the catalyst sample (m_{pd}).

$$r_{Toluene} = \frac{X_{Toluene} \cdot F_{BZA}}{m_{Pd}} \left[mol \cdot s^{-1} \cdot g_{Pd}^{-1}\right] \quad (1)$$

Turnover frequencies were calculated according to Eq 2 by multiplying the rate of production ($r_{Toluene}$) by the molar mass of Pd (M_{Pd}) divided by the apparent metal dispersion.

$$TOF_{Toluene} = \frac{r_{Toluene} \cdot M_{Pd}}{Dispersion} \left[s^{-1}\right] \quad (2)$$

To determine the selectivity performance of the catalysts, selectivity for toluene over benzene was monitored (Eq 3). The intermediate product benzaldehyde was not included in the selectivity calculation because prior work[35] has shown that benzaldehyde formation is rapidly reversible under the reaction conditions, such that benzaldehyde yield drops with increasing benzyl alcohol conversion.

$$Toluene\ Selectivity = \frac{Toluene\ Yield}{Toluene\ Yield + Benzene\ Yield} \quad (3)$$

2.4 Naming Conventions

All samples prepared via metal-first deposition are labeled "XPA/Y%Pd/Al_2O_3." Samples prepared via SAM-first deposition are labeled "Y%Pd/XPA/Al_2O_3." 'XPA' refers to the phosphonic acid SAM used (MPA, ClMPA, or NH_2MPA) while 'Y%' refers to the Pd target weight loading (5%, 1%, or 0.2%).

3. Results and discussion

3.1 Characterization

A series of catalysts was prepared using metal-first deposition (Fig. 1a), where the metal was incorporated onto the metal oxide support via incipient wetness prior to SAM deposition; this is the traditional method for SAM modification of catalysts. A second series of catalysts was prepared using SAM-first deposition (Fig. 1b). Here, incipient wetness impregnation was performed to incorporate the metal onto the SAM-coated surface, allowing the metal to remain free of ligands after deposition on the support. For each series of catalysts, the Pd weight loading and PA functionality were also varied. Weight loadings used include 5 wt%, 1 wt%, and 0.2 wt%. Three different PAs (Fig. 1c) were used for synthesis of the 5 wt% catalyst including chloromethyl phosphonic acid (ClMPA), methyl phosphonic acid (MPA), and aminomethyl phosphonic acid (NH_2MPA). These three PA ligands were chosen because of their varied tail functionalities and compatibility with water. Other PAs including those with long hydrocarbon chains or aromatic groups were found to increase the hydrophobicity of the support to the extent of affecting metal deposition during incipient wetness with aqueous solutions. Prior work has shown that increasing Brønsted acidity contributes to better HDO performance.[20] The ClMPA modifier was previously found to be more acidic than MPA based on temperature programmed

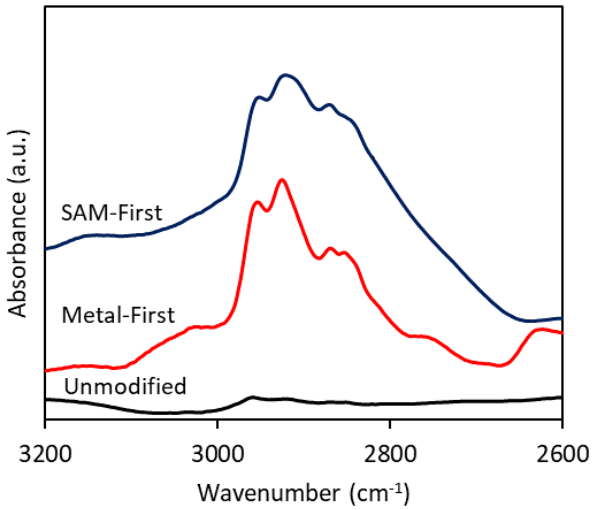

Fig. 3 DRIFTS spectra for unmodified 5%Pd/Al_2O_3 and 5%Pd/Al_2O_3 catalysts modified with NH_2MPA.

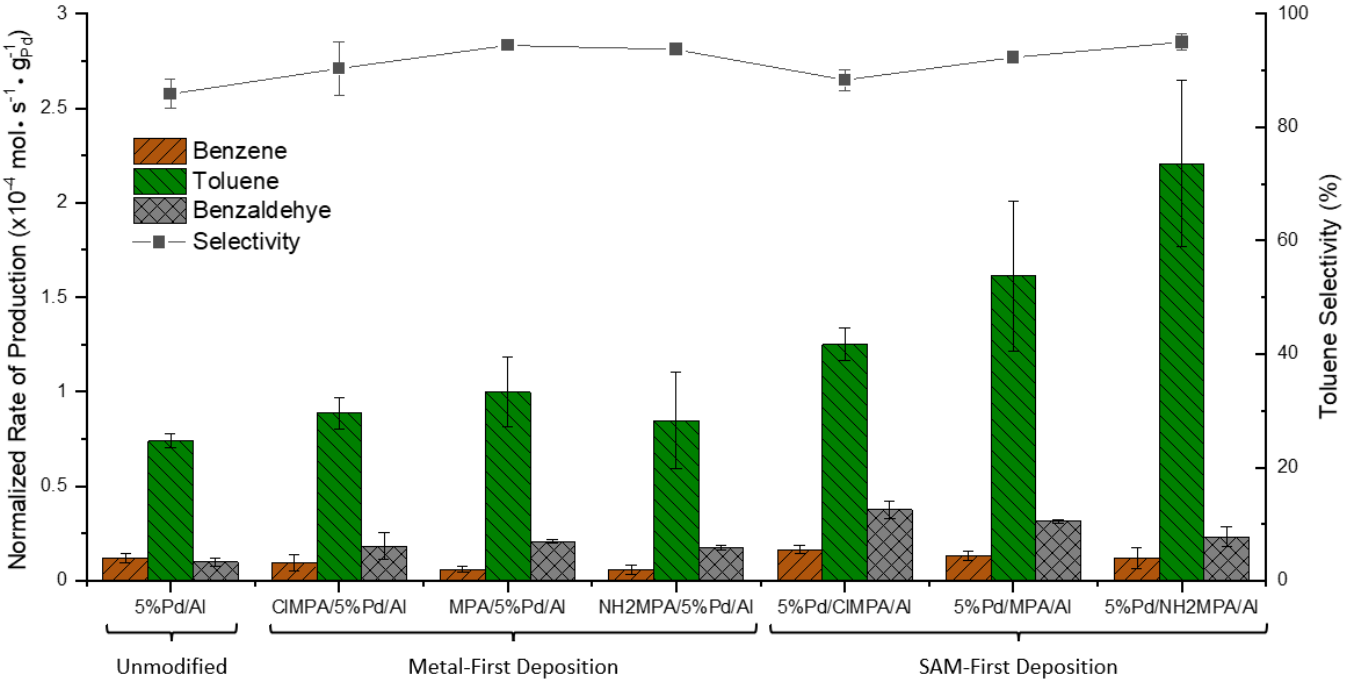

Fig. 4. Benzyl alcohol HDO performance over 5%Pd/Al_2O_3 catalysts modified with ClMPA, MPA, and NH_2MPA through both Metal-First (PA/5%Pd/Al) and SAM-First (5%Pd/PA/Al) deposition.

pyridine DRIFTS experiments and also produced a more active HDO catalyst. Therefore, both ClMPA and MPA were studied to encompass both strongly and moderately acidic PAs. NH_2MPA has also been previously shown to stabilize CO_2 adsorption through an acid / base interaction.[26] While this effect would not apply to benzyl alcohol HDO, preliminary studies showed improved HDO performance using NH_2MPA as a SAM, warranting additional testing.

DRIFT spectra (Fig. 3) and STEM-EDS images (Fig. S1) were collected to confirm that the catalysts synthesized had the intended SAM functionalization, regardless of deposition technique used, SAM used, or Pd weight loading. Representative DRIFT spectra for two different NH_2MPA-modified 5%Pd/Al_2O_3 catalysts (metal-first deposition and SAM-first deposition) and unmodified 5%Pd/Al_2O_3 shown in Fig. 3 demonstrate that SAMs were successfully deposited during both deposition techniques with minor differences in the SAM structure. The absence of C-H stretching peaks for the unmodified catalyst indicate that hydrocarbons were not abundant on the control samples. Meanwhile, C-H stretching peaks clearly appeared in the region of 2800 - 3000 cm^{-1} for 5%Pd/Al_2O_3 after modification with NH_2MPA. Moreover, similar peaks were found in both samples, including asymmetric and symmetric methylene stretches found around 2925 cm^{-1} and 2855 cm^{-1} respectively.[36–38] The presence of similar peaks indicated similar surface functionalization from both deposition techniques It should be noted that the peak locations for the metal-first catalyst were shifted to higher wavenumbers, possibly indicating a more disordered SAM.[33-35] However, the subtle differences in peak location and intensity are difficult to assign to specific structural features of the SAMs near interface sites, especially because the DRIFTS signals are dominated by the SAMs on the metal oxide surface compared to SAMs on the metal. Additional DRIFTS data (Fig. S3) were collected for the catalysts synthesized for Pd loadings of 1 wt% and 0.2 wt% as well as catalysts modified with MPA and ClMPA. Observations with respect to C-H stretching were similar to those from the NH_2MPA-modified 5%Pd/Al_2O_3 catalysts, further supporting the conclusion that catalysts were successfully functionalized with PAs and the different deposition sequences led to similar functionalization, possibly signaling slight differences in SAM ordering depending on the synthesis technique used. Lower Pd weight loadings did not exhibit shifts in wavenumber for metal-first catalysts but still showed differences in selectivity and activity (as discussed below), suggesting that change in SAM structure / ordering is not the major cause of any changes in catalytic behavior.

STEM-EDS imaging was performed on the catalysts to investigate the distribution of Pd and PAs on the surface. Representative images are shown in Fig. S1 for Pd/Al_2O_3 catalysts of varied weight loading, PA, and deposition order. The wide distribution of phosphorous on the catalyst indicated that PAs were well dispersed across the surface, and no noticeable differences were observed between metal-first and SAM-first catalysts. Elemental mapping of an area containing no Pd on ClMPA/5%Pd/Al_2O_3 (Fig. S2) showed significant Cl, suggesting that the tail functionality of the PA is intact.

3.2 Reactivity of metal-first catalysts

To determine the effect of different PA tail functionalities on reactivity, benzyl alcohol HDO was performed on metal-first 5%Pd catalysts modified with the three different SAMs. Activity in terms of rate of production normalized per mass of Pd in the

Table 1: Catalyst Characterization

Catalyst	Pd wt%	Apparent Dispersion (%)[α] from CO Chemisorption	Average Particle Size (nm) from TEM
5%Pd/Al_2O_3	5.0	30 ± 2.7	4.3 ± 1.1
ClMPA/5%Pd/Al_2O_3	5.0	14 ± 1.3	3.4 ± 1.1
5%Pd/ClMPA/Al_2O_3	5.0	24 ± 2.2	3.2 ± 0.5
MPA/5%Pd/Al_2O_3	5.0	12 ± 1.1	-
5%Pd/MPA/Al_2O_3	5.0	26 ± 2.3	2.6 ± 0.3
NH_2MPA/5%Pd/Al_2O_3	5.0	8 ± 0.7	-
5%Pd/NH_2MPA/Al_2O_3	5.0	28 ± 2.5	2.8 ± 0.4
1%Pd/Al_2O_3	1.0	42 ± 3.8	3.9 ± 1.1
ClMPA/1%Pd/Al_2O_3	1.0	24 ± 2.2	-
1%Pd/ClMPA/Al_2O_3	1.0	46 ± 4.1	-
0.2%Pd/Al_2O_3	0.2	92 ± 8.3	3.1[β] ± 1.0
ClMPA/0.2%Pd/Al_2O_3	0.2	36 ± 3.2	3.5[γ] ± 1.2
0.2%Pd/ClMPA/Al_2O_3	0.2	40 ± 3.6	2.7[δ] ± 1.0

α = Apparent dispersions calculated under the assumption of one CO molecule bound to two Pd sites
β = particle size based on the average of 88 particles
γ = particle size based on the average of only 60 particles
δ = particle size based on the average of 134 particles

catalyst (Fig. 4) was modestly increased using metal-first deposition for the various PAs tested, accompanied by a minor increase in toluene selectivity. The increase in activity is attributed to the addition of Brønsted acid sites from the PA, which has been observed to promote the HDO reaction rate.[20,22] Additionally, the higher density of PAs on the Pd surface can prevent the reactant from adopting a flat-lying conformation on well-coordinated terrace sites, restricting the production of the decarbonylation product, benzene,[39] resulting in an even higher toluene selectivity. Although the Brønsted acidity of the PAs increased HDO activity, it is hypothesized that loss of active sites due to blockage by the PAs bound directly to Pd limited the overall production rate compared to the dramatic increase that would be expected. The combination of these two factors resulted in only a modest increase in activity.

To test the site blocking hypothesis, CO chemisorption was performed to estimate active site densities. Apparent dispersions determined using CO chemisorption (Table 1) clearly demonstrated that metal-first PA deposition blocked metal active sites. For all 5%Pd/Al_2O_3 catalysts modified via metal-first deposition (ClMPA/5%Pd/Al_2O_3, MPA/5%Pd/Al_2O_3, and NH_2MPA/5%Pd/Al_2O_3), there was a clear decrease in apparent dispersion from 30% in the unmodified case to 14%, 12%, and 8%, respectively. Apparent dispersion is a measure of the number of unblocked surface sites that are available for the reaction to occur. This is commonly related to the size of the metal nanoparticles, with larger particles exhibiting lower dispersions as there are proportionately fewer surface atoms.[40,41] However, TEM analysis (discussed later in more detail) showed that these modified catalysts did not produce larger particles; in fact, they were somewhat smaller. The likely explanation for this phenomenon is that PA ligands bound directly onto the metal, blocking active sites, which led to less CO adsorbed during chemisorption, and, as a result, lower apparent dispersions.

The CO chemisorption data were used to estimate turnover frequencies (TOFs) for the reactions. As shown in Fig. 5, computed TOFs were significantly higher for metal-first deposition, consistent with a picture where PAs greatly improved the activity of the remaining available sites.

3.3 Reactivity of SAM-first catalysts

Catalysts for each of the three PA functionalities on 5%Pd were also synthesized and tested using SAM-first deposition. Similar to metal-first deposition, SAM-first deposition increased rates of production and selectivity to toluene (Fig. 4) over 5%Pd/Al_2O_3. This increase was again attributed to additional Brønsted acidity provided by the PAs at the interface of the metal and metal oxide support.[20,22] When comparing deposition order, it is clear that SAM-first catalysts exhibited a more substantial increase in the rates of production compared to their metal-first counterparts; this was attributed to a diminished extent of Pd site blocking since PAs should be generally confined to the support. SAM-first catalysts showed an increase in toluene selectivity compared to the unmodified case because of the higher rate of HDO. However, toluene selectivity was slightly lower for ClMPA and MPA SAM-first catalysts compared to metal-first catalysts, ostensibly due to

diminished site-blocking of Pd terrace sites far from the interface; those sites are commonly associated with decarbonylation.[39]

CO chemisorption was again used to determine the apparent dispersions of these catalysts (Table 1). SAM-first catalysts (5%Pd/ClMPA/Al_2O_3, 5%Pd/MPA/Al_2O_3, and 5%Pd/NH_2MPA/Al_2O_3) yield apparent dispersions much closer the 30% found for the unmodified catalyst (24%, 26%, and 28% respectively). Similar results were found for the 1%Pd/Al_2O_3 catalyst modified with ClMPA where metal-first deposition reduced apparent dispersion to 24% while SAM-first deposition left the dispersion (46%) much closer to the unmodified case (42%). In other words, precoating the Al_2O_3 surface with SAMs appeared to result in the ligands existing mostly on the support surface, leaving the metal mostly free of active site blockage, therefore yielding higher rates of production.

Turnover frequency analysis (Fig. 5) for SAM-first catalysts revealed intermediate rates compared to unmodified and metal-first catalysts on a per active site basis, which was attributed to having a mixture of PA-promoted sites (close to the interface) and unpromoted sites (far from the interface). While the catalytic activity of an individual site was higher for metal-first deposition, the drastically decreased dispersion due to site blockage was detrimental to the mass activity of the catalyst. This leads to the conclusion that SAM-first deposition may be the preferred synthesis technique to improve overall activity by improving TOF compared to unmodified catalysts while not substantially decreasing active site availability.

In terms of varying tail functionality, there was no statistically significant difference between the activities for metal-first deposition catalysts. However, it was clear for SAM-first deposition catalysts that the PA used had a significant effect. In terms of activity, it was observed that NH_2MPA > ClMPA while the trends with respect to MPA were within error. Prior work by Zhang et al. has shown that HDO activity correlates with Brønsted acid strength, with ClMPA promoting benzyl alcohol HDO on Pt/Al_2O_3 more than MPA.[20] It should be noted that all of the work in the prior study focused only on the traditional metal-first deposition procedure. With SAM-first deposition the PA tails could also affect Pd particle size / structure (since the PA tail function may influence the metal impregnation process), and this effect could partially mask trends with respect to PA acidity. In fact, SAM-first deposition did appear to change the way that Pd particles were deposited in terms of particle size and site availability depending on which PA was used to precoat the surface. We discuss this point in more detail below.

Experiments were also conducted with lower Pd weight loadings of 1% and 0.2%. Mass activity normalized per mass of Pd (Fig. S4) generally increased as Pd loading decreased as a result of smaller average particle size and increased apparent dispersion. With respect to the different deposition techniques, for 5 wt% and 1 wt% Pd/Al_2O_3, the trend in activity was the same as described above, in which both SAM deposition techniques led to higher activity while SAM-first deposition provided the highest. Conversely, the opposite trend was observed for 0.2%Pd/Al_2O_3 where it appeared that the addition of ClMPA via metal-first deposition did not improve HDO performance and SAM-first deposition gave lower rates. Although the reason for this change in trends at low Pd weight loadings is not clear, it may be related to differences in the distribution of metal particles, clusters, and single atoms for low metal weight loadings. The effect of Pd weight loading is discussed in more detail in the supporting information.

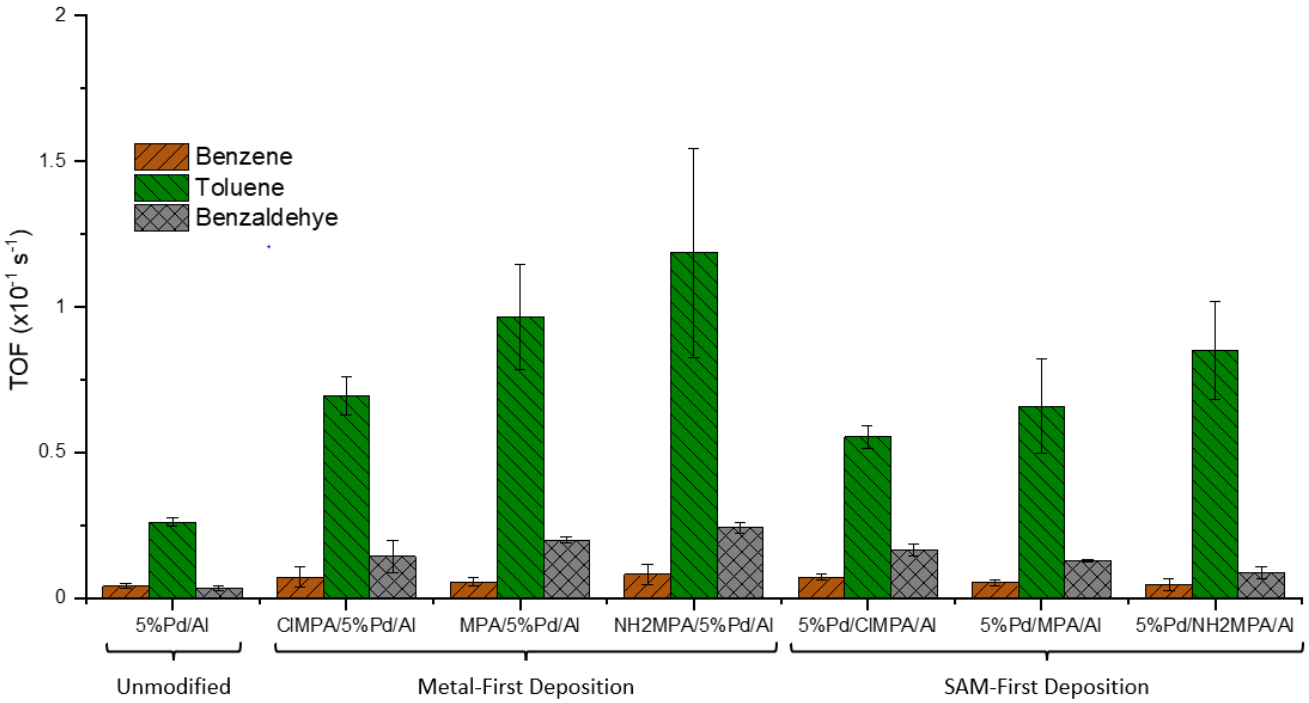

Fig. 5 Turnover frequencies for 5%Pd/Al_2O_3 catalysts modified with ClMPA, MPA, and NH_2MPA through both Metal-First (PA/5%Pd/Al) and SAM-First (5%Pd/PA/Al) deposition.

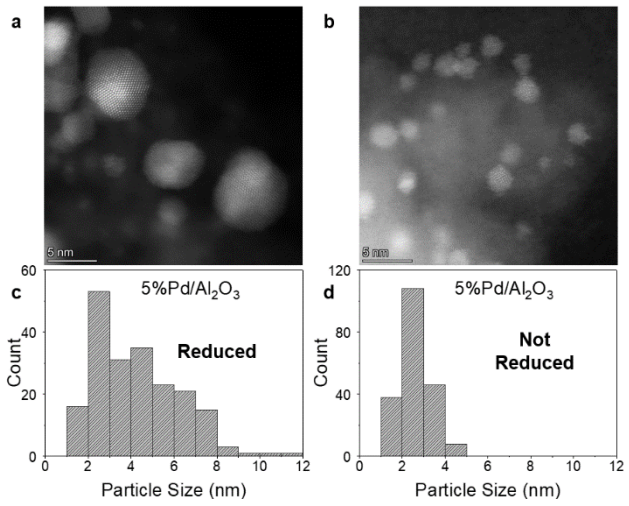

Fig. 6 Representative HAADF-STEM images and particle size distribution for 5%Pd/Al_2O_3 (a)&(c) Reduced at 250 °C for 2h, (b)&(d) Unreduced

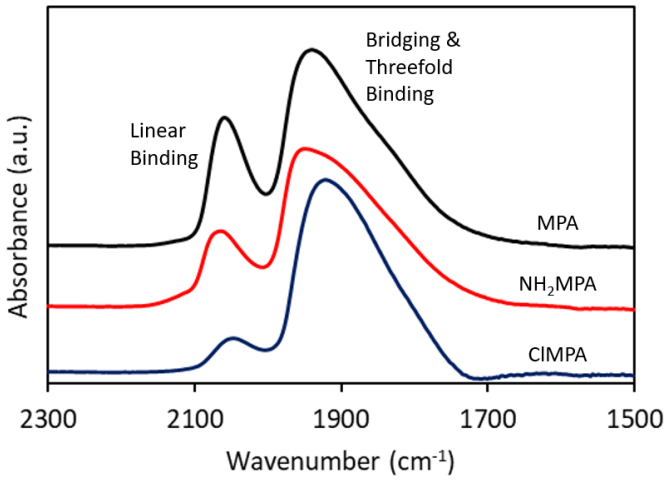

Fig. 7 CO DRIFT spectra for 5%Pd/Al_2O_3 SAM-first deposition catalysts.

3.4 Effect of SAMs on metal deposition

An interesting finding in this study is that SAM-first deposition changed the way that Pd was deposited, particularly for low Pd weight loadings, as apparent dispersion, particle size, and Pd site distribution depended heavily on the PA functionality and deposition sequence used. CO chemisorption results suggested that metal-first catalysts exhibited much lower apparent dispersions than unmodified catalysts, which would be in line with larger Pd particles. However, TEM analysis showed that metal-first catalysts exhibited smaller particles. Thus, SAMs deposited directly onto Pd particles and blocked sites, limiting overall CO uptake during chemisorption and resulting in lower-than-expected apparent dispersions.

The apparent dispersions for SAM-first catalysts were more in line with the unmodified case suggesting that the particles could be about the same size. However, TEM analysis (Table 1) revealed a more complicated scenario, in which Pd average particle size and particle size distribution were affected by the presence and type of SAMs on the surface. Modification with PAs generally led to detection of smaller particles than in the unmodified case, which should theoretically give higher apparent dispersions. This discrepancy can be explained if there is still some site-blocking from the PAs either due to migration of some ligands onto Pd or because PAs on the support could still sterically hinder adsorption onto Pd sites directly at the interface between Pd and Al_2O_3, effectively lowering the number of sites for CO uptake during the chemisorption experiments. Alternatively, PA ligands have been shown to affect the adsorption strength of CO via through-support electronic effects.[26] This could affect the saturation coverage during CO chemisorption measurements and lead to differences in the apparent uptake of CO.

The question remains as to why SAM-first catalysts resulted in smaller particles. One possible explanation is that the smaller particles could be a result of reduced particle agglomeration. To test this, TEM analysis was performed on 5%Pd/Al_2O_3 prior to the reduction pretreatment (Fig. 6), resulting in an average particle size of only 2.6 nm and a particle size distribution with no detected particles larger than 5 nm, in contrast to the reduced 5%Pd/Al_2O_3 which was found to have particles larger than 10 nm. In fact, other unmodified catalysts (1%Pd/ Al_2O_3 and 0.2%Pd/ Al_2O_3) also experience a wide distribution of particle sizes containing unusually large particles (Fig. S7) compared to catalysts modified with PAs. This led to the conclusion that particle growth occurred on the catalysts during the initial reduction at 250 °C, and that SAMs played a role in retarding this growth process. Thus, one possible reason that the PA-modified catalysts exhibit lower average particle sizes and narrower particle size distributions is that the PAs reduce sintering, which has previously been observed for Au/TiO_2[42] and atomically dispersed Rh/Al_2O_3 catalysts.[43] However, it is also interesting to note that for 5%Pd/Al_2O_3 modified with ClMPA, SAM-first deposition resulted in smaller particles than metal-first deposition. Similarly, for 5%Pd/Al_2O_3 catalysts, different PA modifiers resulted in different average particle sizes ranging from 3.2 nm for 5%Pd/ClMPA/Al_2O_3 to 2.6 nm for 5%Pd/MPA/Al_2O_3. The dependence of particle size on deposition method and SAM functionality suggest that the extent of sintering reduction is dependent on the SAM used, or that different tail functionalities influence initial Pd deposition in different ways.

CO DRIFT spectra (Fig. 7) also confirmed a difference in Pd site distribution, which was correlated with Pd particle size, for the 5%Pd SAM-first deposition catalysts. This provides more evidence that precoating the support surface with PAs influenced how Pd was deposited. Infrared peaks were identified for CO bound through bridging and threefold sites (~1900 cm^{-1}) and CO bound to Pd via linear binding (~2050 cm^{-1}).[44–48] The higher proportion of linear binding for 5%Pd/MPA/Al_2O_3 indicated a greater fraction of undercoordinated Pd sites, which was consistent with the TEM result that this modification resulted in smaller average particle sizes compared to 5%Pd/ClMPA/Al_2O_3 and

5%Pd/NH_2MPA/Al_2O_3. No peaks were identified in the 2110-2150 cm^{-1} region related to CO bound to palladium oxide, indicating that all catalysts were fully reduced.[49]

Indeed, the major SAM effects on benzyl alcohol HDO performance observed for SAM-first catalysts may be largely due to changes in particle size and site distribution, rather than differences in Brønsted acidity as originally postulated. For instance, 5%Pd/ClMPA/Al_2O_3 was originally projected to outperform the other catalysts in terms of HDO activity due to higher acidity, yet this catalyst performed worse than 5%Pd/MPA/Al_2O_3 and 5%Pd/NH_2MPA/Al_2O_3. Despite higher Brønsted acidity, the ClMPA precoated surface led to a catalyst with a low fraction of undercoordinated sites and the largest average particle size of the three SAM-first catalysts. Meanwhile, the MPA precoated surface resulted in a catalyst with a high fraction of undercoordinated sites and the smallest average particle size. It is likely that the HDO performance of these catalysts is a function of Brønsted acidity, Pd particle size, and Pd site distribution. The increase in activity due to smaller particles and higher fractions of undercoordinated sites for MPA and NH_2MPA modified catalysts likely outweighs their lower Brønsted acid strength, making these catalysts perform better than the ClMPA-modified case. Although 5%Pd/MPA/Al_2O_3 had smaller particles than 5%Pd/NH_2MPA/Al_2O_3, the latter catalyst still provided the greatest HDO performance possibly due to favorable interactions between the amine function and reactive intermediates.

4. Conclusions

SAM-modified catalysts were synthesized using two deposition sequences (metal-first and SAM-first) and tested for benzyl alcohol HDO. Modification of 5 wt% Pd/Al_2O_3 catalysts with various PAs was found to greatly increase toluene selectivity and activity on a per-site basis. However, deposition of the SAM after metal impregnation resulted in only modest increases to rate of toluene production per mass of catalyst due to site blocking by PAs on Pd. SAM-first deposition, in which the PA was deposited before metal impregnation, allowed for increased TOF compared to unmodified catalysts. However, the real benefit of SAM-first deposition was the increase in rate of toluene production due to increased surface site availability compared to metal-first catalysts, as evidenced by increased apparent dispersion found using CO chemisorption. In addition, precoating the support material with different ligands affected how Pd was deposited onto the surface, resulting in smaller particles compared to metal-first deposition and the unmodified case. For SAM-first deposition, the variations in PA functionality had a minor effect on the rate of production but appeared to lead to different particle sizes depending on the specific PA used. Changes in metal deposition compared to a bare Al_2O_3 support suggest that the effect of the SAMs is quite complex. Nevertheless, depositing SAMs prior to metal deposition appears to provide a viable strategy to design of more active catalysts with minimal site blocking.

Author Contributions

Z.B. conducted the material synthesis, reaction tests, and IR characterization. J.Z. was integral to the conceptualization of the research project. S.Y. conduced STEM-EDS experiments. M.G. conducted CO chemisorption experiments. D.K.S. and J.W.M. supervised the project. All authors discussed results and contributed to the manuscript.

Conflicts of interest

There are no conflicts to declare.

Acknowledgements

The authors acknowledge support the Department of Energy, Office of Science, Basic Energy Sciences Program, Chemical Sciences, Geosciences, and Biosciences Division [Grant No. DE-SC0005239].

References

1 Munnik, P.; de Jongh, P. E.; de Jong, K. P., *Chem. Rev.,* 2015, 115 (14), 6687–6718.
2 Friend, C. M.; Xu, B., *Acc. Chem. Res*., 2017, 50 (3), 517–521.
3 Bridgwater, A. V., *Biomass and Bioenergy*, 2012, 38, 68–94.
4 Griffin, M. B.; Ferguson, G. A.; Ruddy, D. A.; Biddy, M. J.; Beckham, G. T.; Schaidle, J. A., *ACS Catal*., 2016, 6 (4), 2715–2727.
5 Sitthisa, S.; Resasco, D. E., *Catal Lett*., 2011, 141 (6), 784–791.
6 Furimsky, E., *Applied Catalysis A: General*., 2000, 199 (2), 147–190.
7 Robinson, A. M.; Hensley, J. E.; Medlin, J. W., *ACS Catal*., 2016, 6 (8), 5026–5043.
8 Nelson, R. C.; Baek, B.; Ruiz, P.; Goundie, B.; Brooks, A.; Wheeler, M. C.; Frederick, B. G.; Grabow, L. C.; Austin, R. N., *ACS Catal*., 2015, 5 (11), 6509–6523.
9 Chia, M.; Pagán-Torres, Y. J.; Hibbitts, D.; Tan, Q.; Pham, H. N.; Datye, A. K.; Neurock, M.; Davis, R. J.; Dumesic, J. A., *J. Am. Chem. Soc*., 2011, 133 (32), 12675–12689.
10 Wu, D.; Hernández, W. Y.; Zhang, S.; Vovk, E. I.; Zhou, X.; Yang, Y.; Khodakov, A. Y.; Ordomsky, V. V., *ACS Catal*., 2019, 9 (4), 2940–2948.
11 Mortensen, P. M.; Grunwaldt, J.-D.; Jensen, P. A.; Knudsen, K. G.; Jensen, A. D., *Applied Catalysis A: General*, 2011, 407 (1–2).
12 Ranadive, P.; Blanchette, Z.; Spanos, A.; Medlin, J. W.; Brunelli, N., *J Flow Chem*., 2021.
13 Do, P. T. M.; Foster, A. J.; Chen, J.; Lobo, R. F., *Green Chem*., 2012, 14 (5), 1388
14 Newman, C.; Zhou, X.; Goundie, B.; Ghampson, I. T.; Pollock, R. A.; Ross, Z.; Wheeler, M. C.; Meulenberg, R. W.; Austin, R. N.; Frederick, B. G., *Applied Catalysis A: General,* 2014, 477, 64–74.
15 Chen, G.; Xu, C.; Huang, X.; Ye, J.; Gu, L.; Li, G.; Tang, Z.; Wu, B.; Yang, H.; Zhao, Z.; Zhou, Z.; Fu, G.; Zheng, N., *Nature Mater*., 2016, 15 (5), 564–569.
16 Yun, S.; Lee, S.; Yook, S.; Patel, H. A.; Yavuz, C. T.; Choi, M., *ACS Catal*., 2016, 6 (4), 2435–2442.
17 Schoenbaum, C. A.; Schwartz, D. K.; Medlin, J. W., *Journal of Catalysis*, 2013, 303, 92–99.
18 Kahsar, K. R.; Schwartz, D. K.; Medlin, J. W., *J. Am. Chem. Soc*., 2014, 136 (1), 520–526.

19 Wu, D.; Baaziz, W.; Gu, B.; Marinova, M.; Hernández, W. Y.; Zhou, W.; Vovk, E. I.; Ersen, O.; Safonova, O. V.; Addad, A.; Nuns, N.; Khodakov, A. Y.; Ordomsky, V. V., *Nat Catal*., 2021, 4 (7), 595–606.
20 Zhang, J.; Ellis, L. D.; Wang, B.; Dzara, M. J.; Sievers, C.; Pylypenko, S.; Nikolla, E.; Medlin, J. W., *Nat Catal*., 2018, 1 (2), 148–155.
21 Coan, P. D.; Griffin, M. B.; Ciesielski, P. N.; Medlin, J. W., *J. Catal.*, 2019, 372, 311–320.
22 Hao, P.; Schwartz, D. K.; Medlin, J. W., *Appl. Catal. Gen.,* 2018, 561, 1–6.
23 Hao, P.; Schwartz, D. K.; Medlin, J. W., *ACS Catal.*, 2018, 8 (12), 11165–11173.
24 Hoque, E.; DeRose, J. A.; Kulik, G.; Hoffmann, P.; Mathieu, H. J.; Bhushan, B., *J. Phys. Chem. B*, 2006, 110 (22), 10855–10861.
25 Hauffman, T.; Blajiev, O.; Snauwaert, J.; van Haesendonck, C.; Hubin, A.; Terryn, H., *Langmuir*, 2008, 24 (23), 13450–13456.
26 Zhang, J.; Deo, S.; Janik, M. J.; Medlin, J. W., *J. Am. Chem. Soc*., 2020, 142, 11, 5184–5193.
27 Coan, P. D.; Ellis, L. D.; Griffin, M. B.; Schwartz, D. K.; Medlin, J. W., *J. Phys. Chem. C* **2018**, *122* (12), 6637–6647.
28 Coan, P. D.; Farberow, C. A.; Griffin, M. B.; Medlin, J. W., *ACS Catal.* **2021**, *11* (6), 3730–3739.
29 Dietrich, H.; Schmaltz, T.; Halik, M.; Zahn, D., *Phys. Chem. Chem. Phys.* **2017**, *19* (7), 5137–5144.
30 Luschtinetz, R.; Oliveira, A. F.; Frenzel, J.; Joswig, J.-O.; Seifert, G.; Duarte, H. A., *Surf. Sci.* **2008**, *602* (7), 1347–1359.
31 D'Andre, S. C.; Fadeev, A. Y., *Langmuir* **2003**, *19* (19), 7904–7910.
32 Helmy, R.; Fadeev, A. Y., *Langmuir* **2002**, *18* (23), 8924–8928.
33 Fagherazzi, G.; Canton, P.; Riello, P.; Pernicone, N.; Pinna, F.; Battagliarin, M., *Langmuir*, 2000, 16 (10), 4539–4546.
34 Canton, P.; Fagherazzi, G.; Battagliarin, M.; Menegazzo, F.; Pinna, F.; Pernicone, N., *Langmuir*, 2002, 18 (17), 6530–6535.
35 Lien, C.-H.; Medlin, J. W., *J. Phys. Chem. C*, 2014, 118 (41), 23783–23789.
36 Nuzzo, R. G.; Dubois, L. H.; Allara, D. L., *J. Am. Chem. Soc*., 1990, 112 (2), 558–569.
37 Wiberley, S. E.; Bunce, S. C.; Bauer, W. H., *Anal. Chem*., 1960, 32 (2), 217–221.
38 Snyder, R. G.; Hsut, S. L.; Krimm, S., *Spectrochimica Acta*, 1977, 34A, 395—406.
39 Luschtinetz, R.; Oliveira, A. F.; Duarte, H. A.; Seifert, G., *Z. anorg. allg. Chem*. 2010, 636 (8), 1506–1512.
40 Park, J.-S.; Vo, A. N.; Barriet, D.; Shon, Y.-S.; Lee, T. R., *Langmuir*, 2005, 21 (7), 2902–2911.
41 Shin, H. S.; Kim, J. H.; Kim, S. B.; Jung, Y. M., *Langmuir*, 2007, 23 (21), 10567–10572.
42 Pang, S. H.; Schoenbaum, C. A.; Schwartz, D. K.; Medlin, J. W., *Nat Commun*., 2013, 4 (1), 2448.
43 Huo, J.; Johnson, R. L.; Duan, P.; Pham, H. N.; Mendivelso-Perez, D.; Smith, E. A.; Datye, A. K.; Schmidt-Rohr, K.; Shanks, B. H., *Catal. Sci. Technol*., 2018, 8 (4), 1151–1160.
44 Dobrezberger, K.; Bosters, J.; Moser, N.; Yigit, N.; Nagl, A.; Föttinger, K.; Lennon, D.; Rupprechter, G., *J. Phys. Chem. C*, 2020, 124 (43), 23674–23682.
45 Jenkins, A. H.; Musgrave, C. B.; Medlin, J. W., *ACS Appl. Mater. Interfaces*, 2019, 11 (44), 41289–41296.
46 Zhang, J.; Asokan, C.; Zakem, G.; Christopher, P.; Medlin, J. W., *Green Energy & Environment*, 2021, https://doi.org/10.1016/j.gee.2021.01.022.
47 Xu, J.; Ouyang, L.; Mao, W.; Yang, X.-J.; Xu, X.-C.; Su, J.-J.; Zhuang, T.-Z.; Li, H.; Han, Y.-F., *ACS Catal*., 2012, 2, 261−269.
48 Tiznado, H.; Fuentes, S.; Zaera, F., *Langmuir*, 2004, 20, 10490-1049.
49 Tessier, D.; Rakai, A.; Bozon-Verduraz, F., *J. CHEM. SOC. FARADAY TRANS*., 1992, 88(5), 741-749.
50 Gregorio, F. D.; Bisson, L.; Armaroli, T.; Verdon, C.; Lemaitre, L.; Thomazeau, C., *Applied Catalysis A: General*, 352 (2009) 50–60.
51 Benkhaled, M.; Morin, S.; Pichon, C.; Thomazeau, C.; Verdon, C.; Uzio, D., *Applied Catalysis A: General*, 312 (2006) 1–11.
52 Jang, E. J.; Lee, J.; Oh, D. G.; Kwak, J. H., *ACS Catal*., 2021, 5894–5905.